

# Frequency response improvement of a two-port surface acoustic wave device based on epitaxial AlN thin film

Junning Gao<sup>1,2</sup>, Zhibiao Hao<sup>3</sup>, Yi Luo<sup>3</sup> and Guoqiang Li<sup>1,2</sup>

1 China State Key Laboratory of Luminescent Materials and Devices, School of Materials Science and Engineering, South China University of Technology, Guangzhou, 510641, China

2 Engineering Research Center on Solid-State Lighting and its Informationisation of Guangdong Province, South China University of Technology, Guangzhou, 510641, China

3 Tsinghua National Laboratory for Information Science and Technology, Department of Electronic Engineering, Tsinghua University, Beijing, 100084, China

Email: msjngao@scut.edu.cn, zbhao@tsinghua.edu.cn, luoy@tsinghua.edu.cn, msgli@scut.edu.cn

**Abstract.** This paper presents an exploration on improving the frequency response of the symmetrical two-port AlN surface acoustic wave (SAW) device, using epitaxial AlN thin film on (0001) sapphire as the piezoelectric substrate. The devices were fabricated by lift-off processes with Ti/Al composite electrodes as interleaved digital transducers (IDT). The impact of DL and the number of the IDT finger pairs on the frequency response was carefully investigated. The overall properties of the device are found to be greatly improved with DL elongation, indicated by the reduced pass band ripple and increased stop band rejection ratio. The rejection increases by 8.3 dB when DL elongates from  $15.5\lambda$  to  $55.5\lambda$  and 4.4 dB further accompanying another  $50\lambda$  elongation. This is because larger DL repels the stray acoustic energy out of the propagation path and provides a cleaner traveling channel for functional SAW, and at the same time restrains electromagnetic feedthrough. It is also found that proper addition of the IDT finger pairs is beneficial for the device response, indicated by the ripple reduction and the insertion loss drop.

## 1. Introduction

Surface acoustic wave (SAW) with two-port structure consisting of two interleaved digital transducers (IDT) is of paramount importance in the SAW device family because it can be the basic configuration for the SAW delay line and bandpass device [1, 2]. The applications are wide spread in wireless communication and signal processing system such as radar, Wifi, Bluetooth, and navigation. When applying a sensing medium between the two IDTs, the two-port SAW device can work as sensor, which has been under thrust interest due to its great potential in medical, bio, and materials analysis [3-6].

The center frequency of a SAW device is the outcome of the sound velocity divide by sound wave length. AlN has the highest sound velocity among piezoelectric materials, which makes it a great candidate for high frequency application and less challenging for lithography process. It is favored among other piezo materials also for its superior physical, chemical and mechanical properties [7-12]. In addition for wireless communication, high operation frequency is favored for sensors as well



because the penetration depth of SAW decreases with increasing frequency allowing more adequate interaction between the target and the SAW, thus improve the sensitivity [3].

For a highly functional two-port SAW device, great transmission properties mainly featured as large stop band rejection and small pass band ripple are crucial. Materials imperfections and improper device structure are generally the source of inferior frequency response. Single crystalline AlN film that is solely (0001) oriented along the surface normal and has small roughness is highly desirable for device fabrication. This is because the piezoelectric axis of AlN is along (0001) orientation and surface fluctuations and grain boundaries behave as acoustic wave reflection centers [13-15].

Delay length (DL) between the two IDTs is designed normally out of two considerations. The first is that it needs to be kept short to minimize the material-induced insertion loss and impedance. The second is that for delay line device it determines the delay time because the length between the two IDTs determines the travelling distance of the induced acoustic wave [12, 16]. To the best of our knowledge, the impact of DL on the overall frequency response of the device has not been reported, though we find it has significant influence. Besides, the number of finger pairs is also very important since it affects the resonance amplitude and determines the band width of the device. However, the addition of fingers enlarges the device size which increases the cost. Therefore, these parameters must be thoroughly explored and carefully leveled to reach optimized device performance and keep high cost-effectiveness.

In the presented research, two-port SAW devices have been fabricated on (0001) AlN single crystalline thin films grown by molecular beam epitaxy (MBE), and the device frequency response with an emphasis on the influence of DL and the number of finger pairs have been investigated in detail.

## 2. Experiments

The epitaxial AlN thin film was grown on (0001) sapphire substrate by using MBE with the similar procedure described in [17]. The surface morphology of the epi-wafer was assessed by a PSIA XE-100 atomic force microscopy (AFM). The films are (0001) oriented having HWHM of 131 arcsec for their (0001) X-ray diffraction rocking curves. All of the films in use have the same thicknesses of 1  $\mu\text{m}$ . The two-port SAW devices were fabricated by lift-off processes. The AlN/sapphire wafer was first cleaned to remove organic and inorganic contaminants, then spin coated with AZ5214 photoresist. After being baked on a hot plate, the wafer was subjected to lithography using a SUSS MJB3 lithography machine. After exposure, the wafer was immersed into the developer solution to develop the pattern. Then it was placed onto the stage of a DC and RF bi-functional electrode sputtering equipment, where Ti/Al composite electrode was sputtered. The Ti bottom layer was RF sputtered and the thickness was controlled to be 10 nm, and the Al top layer was DC sputtered and the thicknesses were controlled to be around 110 nm. The process was completed on forming the IDT electrodes through removing the left photoresist in acetone. The optical microscopic image was taken by OLYMPUS microscope and the frequency response was measured by Agilent 8722ET network analyzer.

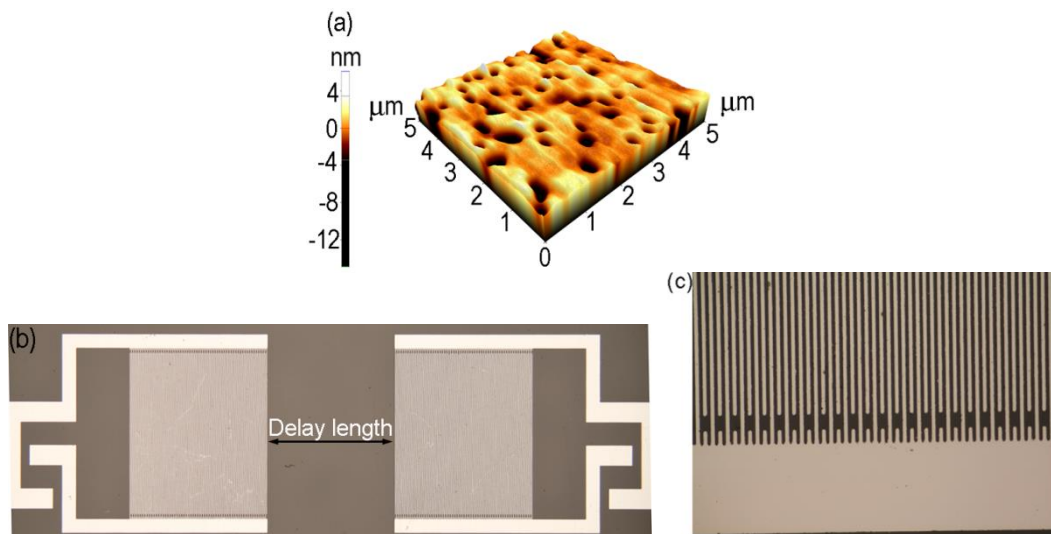
## 3. Results and discussion

### 3.1. Morphology of the device

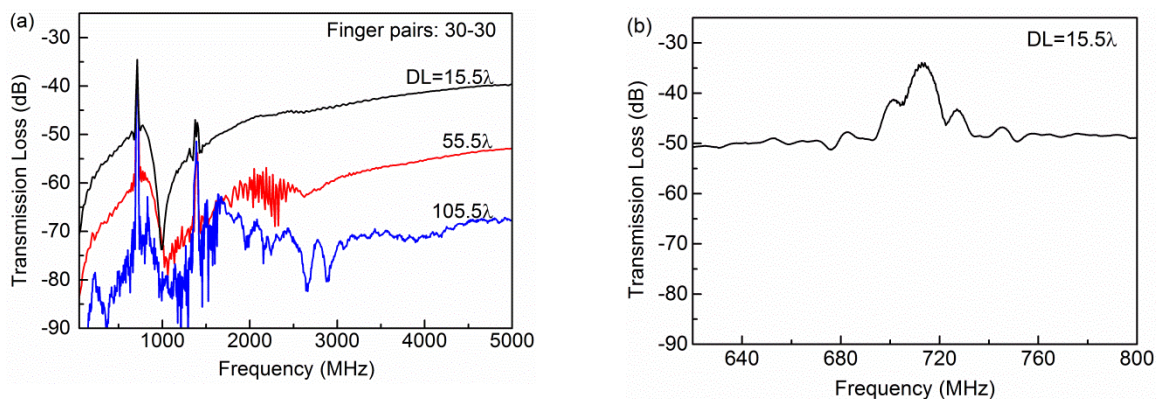
Figure 1 (a) shows the AFM image of the AlN film surface. The root mean square roughness of the film is 1.8 nm. Figure 1 (b) gives an overlook of the device structure showing by microphotograph image. The SAW device is symmetric having one input and one output uniform IDT with each consisting of interleaved fingers, bus bar, and GSG pad for electric loading and detecting. The pads are spaced with standard 150  $\mu\text{m}$  center-to-center distance. Figure 1 (c) exhibits a magnified part of the IDT with details of the fingers and the bus bar. For all devices discussed in this paper, the aperture is 560  $\mu\text{m}$ , and the finger width is uniformly 2  $\mu\text{m}$ , the metallization ratio is 0.5, the IDT period is therefore 8  $\mu\text{m}$  which defines the acoustic wave length as 8  $\mu\text{m}$ .

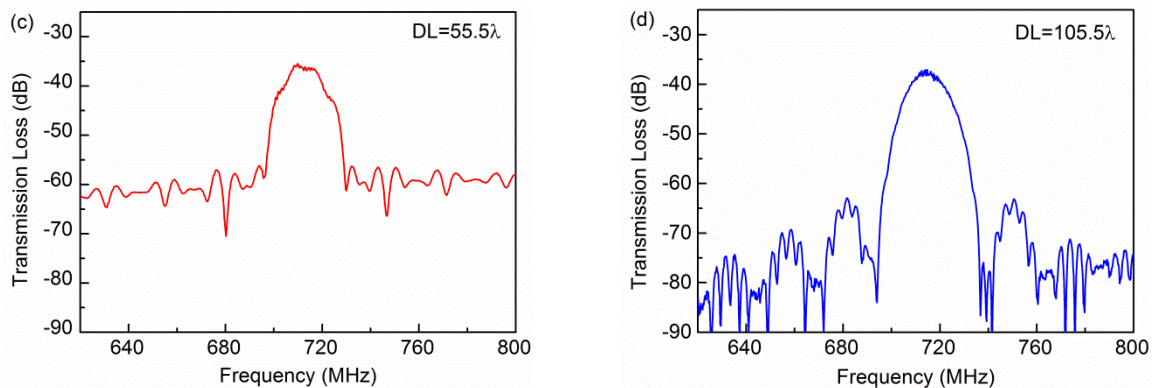
### 3.2. Delay length influence on SAW device performance

Figure 2 shows the frequency response of the two-port SAW devices having 30 pairs of fingers with different DL. Figure 2 (a) exhibits the global transmission loss S<sub>21</sub> spectra of the devices in the range from 50 MHz to 5 GHz, where all three exhibiting two pass bands with one centered at 714 MHz and the other at 1392 MHz. Figure 2 (b), (c) and (d) give detail profile of the three fundamental mode pass bands. The stop band rejection ratio of the device with  $15.5\lambda$  DL is 12.4 dB, it grows 8.3 dB with the first  $50\lambda$  of DL extension and another 4.4 dB with  $50\lambda$  more. The insertion loss of the device with  $15.5\lambda$  DL is 34.4 dB, it rises slightly by 1.1 dB when DL increases  $50\lambda$ , and 2.6 dB further with another  $50\lambda$  distance hopping. It is therefore can be concluded that the stop band rejection ratio increase with DL with slight sacrifice of the pass band insertion loss. It is also worth noting that the pass band ripple is reduced significantly when DL is increased. Following the ripple decrease, the peak shape in Figure 2 (d) is able to match with the theoretically expected Bell shaped function for symmetrical two-port IDT SAW device [19].



**Figure 1.** (a) AFM image of the AlN film surface, the microscopic images of the device (b) an overall view and (c) a local detailed view.





**Figure 2.** Transmission loss of the two-port SAW devices with 30 pairs of fingers: (a) the global transmission loss with different DLs; detailed frequency response of the fundamental mode resonances with DL of (b)  $15.5\lambda$ , c)  $55.5\lambda$  and (d)  $105.5\lambda$ .

Figure 3 presents the pass band profile comparison between  $1/8\lambda$  DL shifting, namely,  $\pi/4$  phase shift. Illustrated by the almost overlapping spectrum in both Figure 3 (a) and Figure 3 (b), the frequency response shows highly resemblance before and after  $1/8\lambda$  shifting of DL, indicating that the relative phase variation of the two IDTs has trivial impact on the frequency domain of the resonance.

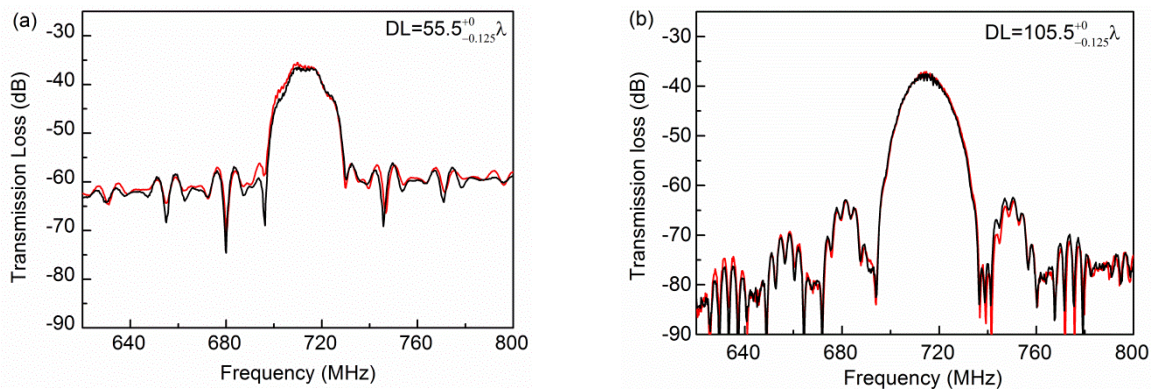


**Figure 3.** Frequency responses comparison of the fundamental mode resonance with  $1/8\lambda$  of DL shifting: (a)  $55.5\lambda$  and (b)  $105.5\lambda$ .

The output of a two-port SAW device is the convolution of the frequency responses of the input IDT and the output IDT. The input IDT converts the incoming electric signal to acoustic wave through inverse piezoelectric effect, the wave then travel to the output IDT where it is converted back to electric signal by piezoelectric effect. The input signal with frequencies that match the eigen frequencies of the device will be picked up and passed, while the rest will be attenuated. When loaded, IDT generates both surface and bulk waves, those that are able to induce resonance are enhanced while the rest dissipate. When the travelling wave meet the edge of the IDT, a part of its energy will be reflected due to the acoustic impedance discontinuity, which can cause damaging second order effect. Bulk wave energy density dissipation is inversely proportional to the distance from the source in the order of  $-0.5$ , hence it decreases rapidly with distance [19, 20]. Larger DL can provide more adequate space for the dissipation of the detrimental acoustic energy such as bulk wave and reflected surface wave and thus repel them out of the travelling path of functional surface wave, providing a cleaner cavity for surface wave resonating. That is why SAW device with larger DL shows improved pass band frequency response. Another important factor that could influence on the properties of SAW delay line device is the electromagnetic feedthrough between the two IDTs, which should be restrained by longer DL between the two IDTs as well. It has found proof in the fact that when having



the same device configuration, device with smaller center frequency always reaches its optimum response at smaller DL distance as reported in another research by the authors [21].

However, larger DL elongates the propagation distance for SAW, which results in larger insertion loss, as shown by the insertion loss increase tendency with DL, and longer delay time. Besides, size augment brought by DL elongation may harm the flexibility and increases the cost of the device. It is therefore suggested that DL should be set at optimized length weighing both the performance and cost of the device.

### 3.3. Influence of the finger pairs number on the device performance

A very important factor impacting on the performance of SAW device is the number of finger pairs. The curves in Figure 4 present the rejection ratio and insertion loss (Figure 4 (a)) as functions of the finger pairs number. It is learned that the out of band rejection increases as the fingers number increases, and it rises to a plateau eventually. The insertion loss, on the other hand, exhibits a slower overall tendency of drop as the number of fingers is added, and reaches a saturation stage in the end. Both two curves state that the device performance grows better with increasing finger pairs and there is a saturation state for this growth. As indicated in the last section, the device performance can be affected by both stray acoustic wave energy and electromagnetic feedthrough. When keeping the number of finger pairs as the only variation parameter, the influence of feedthrough is ruled out. This behavior shown in Figure 4 illustrate that the proper increase of the fingers number is suitable for improving the performance of SAW delay line devices, especially when considering that DL decides the delay time. Further, the bandwidth of the SAW delay line varies inversely with the number of the pairs, as shown by curves in Figure 4 (b). The theoretically expected value was calculated by equation (1) [19], where  $N$  is the pair number, and  $f_0$  is the center frequency of the device. The bandwidth of the device with 10 pairs is left out because the passband ripple is too large to provide the necessary precision for data extraction.

$$BW_{-3dB} = \frac{0.866}{N} f_0 \quad (1)$$

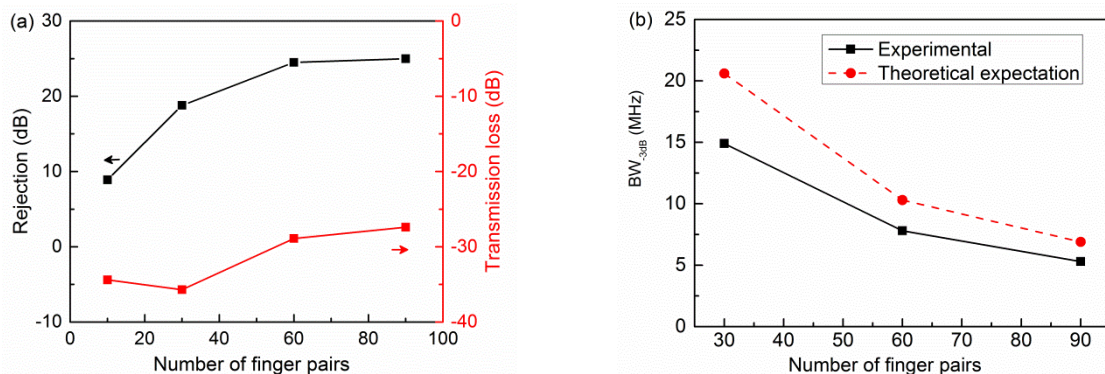


**Figure 4.** The influence of the number of finger pairs on the frequency response: (a) transmission loss and rejection, and (b) 3-dB bandwidth. The devices are all with center frequencies of 714 MHz and DLs of  $55.5\lambda$ .

## 4. Conclusion

Two-port symmetrical AlN SAW device using epitaxial AlN thin film on (0001)sapphire has been fabricated by lift-off process with Ti/Al composite electrodes as IDT. The overall properties of the device can be greatly improved by DL elongation, indicated by the reduced pass band ripple and increased stop band rejection ratio. This is because larger DL provides larger room for nonfunctional acoustic energy dissipation and thus providing cleaner path for functional SAW transmission and better cavity for resonance, and restrains electromagnetic feedthrough as well. It is also found that proper addition of the IDT finger pairs improves the device response, and there is a plateau for this improvement. The reason for this behavior also lies in the fact that more fingers provide better resonance for acoustic waves and rule out stray resonance out of the device.

Since longer distance increase delay time and the size of the device, while more fingers burden fabrication process and increase size as well, there should be a careful weighting in the design of SAW delay line devices.

## 5. References

1. W. C. Wilson and G. M. Atkinson, in 1st Order Modeling of a SAW Delay Line using MathCAD, [Online]. <http://ntrs.nasa.gov/archive/nasa/casi.ntrs.nasa.gov/20070016024.pdf>: Nasa\_Ntrs, 2007, p.6.
2. E. Blampain, O. Elmazria, T. Aubert, et al., IEEE Sensors J. **13**, 4607-4612 (2013).
3. T. M. Gronewold, Anal Chim Acta **603**, 119-128 (2007).
4. J. Luo, P. Luo, M. Xie, et al., Biosens Bioelectron **49**, 512-518 (2013).
5. T. Nomura and A. Saitoh, in *Proc. IEEE Sensors 2002*, Tokyo, Japan, 507-510 (2002).
6. M. Jo, K. J. Lee, and S. S. Yang, Sensor Actuat. A-Phys. **210**, 59-66 (2014).
7. S. Fujii, S. Kawano, T. Umeda, et. al, in *Proc. IEEE International Ultrasonics Symposium*, Beijing, 1916-1919, (2008).
8. O. Elmazria, V. Mortet, M. E. Hakiki, et. al, IEEE T Ultrason. Ferr. **50**, 710-715 (2003).
9. C.-M. Lin, Y.-Y. Chen, V. V. Felmetzger, D. G. Senesky, and A. P. Pisano, Adv. Mater. **24**, 2722-2727 (2012).
10. T. Manzanque, J. Hernando, L. Rodríguez-Aragón, et al., Microsyst. Technol. **16**, 837-845 (2010).
11. E. Blampain, O. Elmazria, T. Aubert, et. al, IEEE Sensors J. **13**, 4607-4612 (2013).
12. J. Zhou, M. DeMiguel-Ramos, L. Garcia-Gancedo, et al., Sensor Actuat. A- Chem. **202**, 984-992 (2014).
13. V. Mortet, M. Nesladek, J. D'Haen, et al., Phys. Stat. Sol. A **193**, 482-488 (2002).
14. A. Ababneh, M. Alsumady, H. Seidel, et al., Appl. Surf. Sci. **259**, 59-65 (2012).
15. W. C. Shih and Z. X. Zoh, Ferroelectrics **459**, 52-62 (2014).
16. S. Fujii, Phys. Stat. Sol. A **208**, 1072-1077 (2011).
17. R. Fan, H. Zhi-Biao, Z. Chen, et. al, Chin. Phys. Lett. **27**, 068101 (2010).
18. M. B. Assouar, O. Elmazria, M. Elhakiki, et. al, J. Vac. Sci. Technol. B **22**, 1717 (2004).
19. A. A. Oliner, "Acoustic Surface Waves" in *Topics in Applied Physics*, (Springer-Verlag Berlin Heidelberg, New York, 1978).
20. J. W. Grate and G. C. Frye, Sensors Update **2**, 37-83 (1996).
21. J. Gao, Z. Hao, Y. Luo. Func. Mater. Lett. **9**, 1650034 (2016).

## Acknowledgments

The author appreciates the financial support by the National Basic Research Program of China (Grant No.2013CB632804), the National Natural Science Foundation of China (Grant Nos. 51602105, 61176015, 61176059, 61210014, 61321004 and 61307024), Natural Science Foundation of Guangdong, China (Grant No. 2017A030313331), the Fundamental Research Funds for the Central Universities (Grant No. F040402), the High Technology Research and Development Program of China (Grant No. 2012AA050601), and the China Postdoctoral Science Foundation.